AIAA JOURNAL
Vol. 42, No. 1, January 2004

Technical Note

TECHNICAL NOTES are short manuscripts describing new developments or important results of a preliminary nature. These Notes cannot exceed six manuscript pages and three figures; a page of text may be substituted for a figure and vice versa. After informal review by the editors, they may be published within a few months of the date of receipt. Style requirements are the same as for regular contributions (*see inside back cover*).

Reynolds Stresses Around the Wheels of a Simplified Four-Wheel Landing Gear

Barry S. Lazos*
NASA Langley Research Center, Hampton, Virginia 23681

Introduction

WITH the significant reduction of jet-engine noise levels in recent years, airframe noise sources have become increasingly important to overall aircraft noise. Three regions of significant airframe noise production are the slats, flaps, and landing gear. For some aircraft, such as the Boeing 777, landing gear can be a dominant airframe noise source (Sen, R., private communication, 1996). Although the signature of landing-gear noise varies between aircraft, it is generally noted to cover a broad range of frequencies resulting from flow interactions with components that range in size from the order of a millimeter to a meter.

Acoustic measurements can provide important information about the noise signature of a particular landing-gear configuration, but a priori knowledge of a configurations aeroacoustics is desirable for design purposes. For this reason attempts are made to theoretically or computationally determine landing-gear noise characteristics. However, to evaluate noise production accurately using flow-physics-based calculations, one must be confident of the accuracy of the calculations. Hedges et al.[1] recently performed calculations of the flowfield around a simplified four-wheel landing-gear configuration with the experimental measurements of Lazos.[2] Two different and distinct calculation methods were used: detached-eddy simulation (DES), which is a hybridization of large-eddy simulation (LES) and Reynolds-averaged Navier–Stokes (RANS), and conventional unsteady Reynolds-averaged Navier–Stokes (URANS). The authors found that DES performs somewhat better than URANS and "appears promising for noise prediction up to some frequency limit."

To further improve computational models of the flow around landing gear, more experimental data are preferred, especially rms or averaged unsteady quantities such as Reynolds stresses. In particular such information could be used to determine if the DES code just mentioned was switching at the proper location from a RANS to an LES calculation. The current study is a follow-on to the two previous studies of Lazos.[2,3] The model is a simplified four-wheel configuration scaled to a Boeing 757 main landing gear. All extraneous dressings were eliminated in order to concentrate on the flow characteristics around the wheels. Tests were conducted at a Reynolds number based on wheel diameter of 6×10^5. Digital particle image velocimetry (DPIV) data were acquired in a plane bisecting the in-line wheels in which three components of Reynolds stress were calculated. Although a limited number of velocity samples were acquired at each data location, the results are expected to be useful for the determination of potential regions of noise generation and for comparison with computational-fluid-dynamics results.

Experimental Setup and Data Reduction

Experiments were conducted in the Basic Aerodynamics Research Tunnel[4] at the NASA Langley Research Center. This facility is an open-circuit wind tunnel with a test-section area of 71×102 cm and a length of 305 cm. The model used in the present study is a simplified generic configuration of a four-wheel landing gear, the same one used in two previous reports.[2,3] A full description of the geometry is given in Ref. 2. The model was positioned such that its lateral center coincided with the lateral center of the tunnel. The wheel centers of the model were positioned at the vertical center of the wind tunnel. Model blockage was approximately 15%. Tunnel freestream velocity was set at 29 m/s to provide a Reynolds number based a wheel diameter of 6×10^5. Reference 4 provides detailed information on tunnel flow quality and indicates that turbulence levels are below 0.1% at near-maximum freestream velocity.

DPIV images were acquired in a single plane surrounding two in-line wheels and was laterally positioned along the center of the wheels. The data plane was separated into 160 quadrants that measured 36×36 mm, each overlapping its neighbors by 4 mm. In each quadrant at least 100 image pairs were acquired. Interrogation of image pairs resulted in 60×60 arrays of instantaneous u- and w-component velocity vectors with a spatial resolution of 0.57 mm.

To calculate the Reynolds-stress values, the mean u and w components of velocity were first determined. In each of the 160 quadrants, the 100 60×60 vector arrays were averaged together, and the data were remapped to a contiguous 676×1236 vector plane surrounding the wheels. Improvements to mean values were made by spatially averaging the vector data. At each vector location the surrounding vectors within a 2.5-mm radius were averaged. So, while grid spacing of the vectors is 0.57 mm, each vector represents an average of its neighbors within the 2.5-mm radius. Reynolds-stress values were also calculated using spatial averaging within a 2.5-mm radius.

For a detailed description of the equipment used and the interrogation procedure, see Lazos.[2] Beyond that, refinement of the data was accomplished by filling in locations where velocity values could not be discerned, using multiple linear regression as described in Landreth and Adrian.[5]

Results and Discussion

As mentioned in Lazos,[2] changes in the mean flow state are apparent from the uw-velocity vector data at locations between the wheels. These changes were hypothesized to result from the the motion of a nonstationary vortex that persists on the ground side of the wheel vertical midplane. It was speculated that this vortex results in ground-directed noise as turbulent eddies are scrubbed against the wheels. Figure 1 highlights a dominant mean flow state in the DPIV data plane bisecting the in-line wheels. This figure was generated using line integral convolution and is identical to Fig. 5 in Ref. 2, where further consideration is given to the mean flow characteristics around the wheels. In the figure flow direction is readily apparent with several streamlines between the wheels highlight in white. Velocity magnitude is represented by coloration. Both separation and attachment locations highlighted in the figure were

Received 27 January 2003; revision received 4 August 2003; accepted for publication 20 August 2003.

*Research Scientist, Flow Modeling and Control Branch.

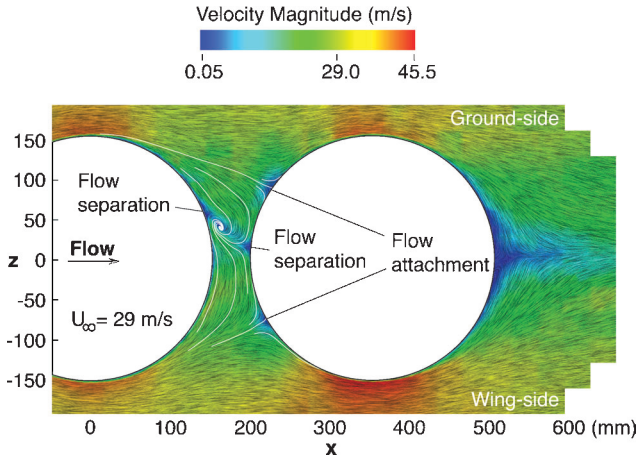

Fig. 1 Velocity magnitude and direction in DPIV data plane. Streamlines between wheels are highlighted in white.

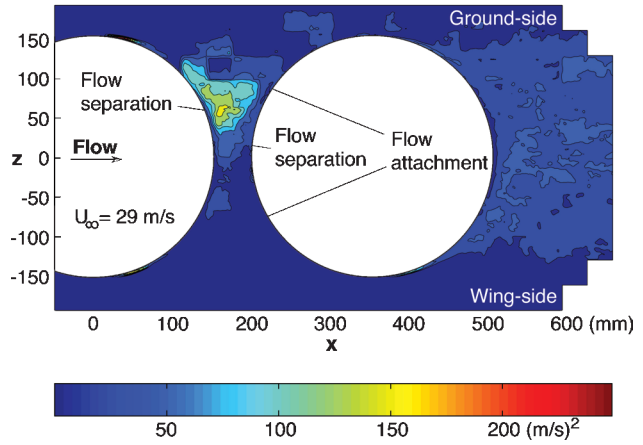

Fig. 2 Reynolds-stress component $\overline{u'^2}$ in a plane bisecting the in-line wheels.

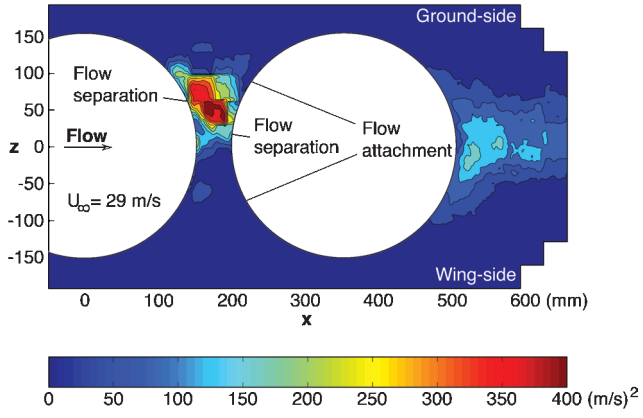

Fig. 3 Reynolds-stress component $\overline{w'^2}$ in a plane bisecting the in-line wheels.

determined using streamline tracing. Note that in Fig. 1, as well as in all subsequent figures, the ground side of the wheels is on the top, and the wing side is on the bottom. This upside-down configuration is used because it is consistent with the orientation of the model in the wind tunnel.

Figures 2, 3, and 4, respectively, show the Reynolds-stress components $\overline{u'^2}$, $\overline{w'^2}$, and $\overline{u'w'}$ in the DPIV data plane. Here the prime indicates a fluctuating quantity, and the overbar indicates the mean. In Fig. 2 the $\overline{u'^2}$ component is observed to reach its maximum value along both sides of the fore wheel surface just downstream of the

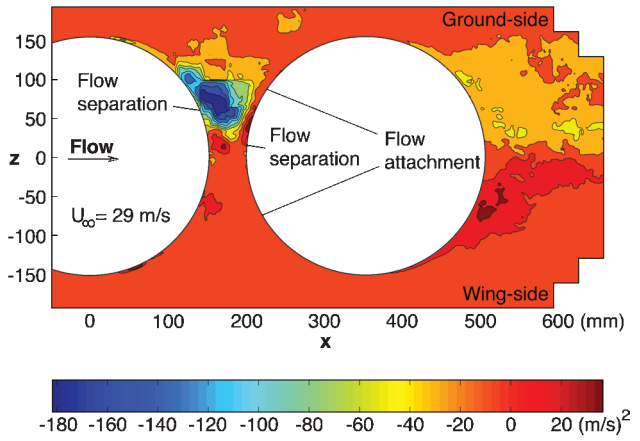

Fig. 4 Reynolds-stress component $\overline{u'w'}$ in a plane bisecting the in-line wheels.

wheel vertical centerline ($x = 0$). These locations, identified by the yellow arrows in the figure, coincide well with the separation and turbulent reattachment regions observed in the oil-flow-visualization images of Lazos.[3] The other most significant region of Reynolds stress in Fig. 2 is the ground side of the wheel gap, just behind the fore wheel. Figures 3 and 4 show that the $\overline{w'^2}$ and $\overline{u'w'}$ components of turbulence are also large in this region. A statistical analysis shows that in this region of high turbulence intensity the w component of velocity has a mean value of approximately 3 m/s and a standard deviation of 20 m/s. The maximum and minimum values of the transverse velocity component are 60 and -48 m/s in this region, up to two times the freestream value.

The preceding turbulence results show that the gap between the wheels is a region of substantial turbulent activity. It is also significant to note that turbulent activity is greatest on the ground side of the wheel horizontal midplane. This suggests that it could be an important contributor to ground-directed landing-gear noise, particularly when the gear consists of more than one wheel set. Currently only speculation can be given concerning solutions to this potential noise source, but the primary culprit appears to be the flow through the wheel gap and the resulting mixing. For the current model the center support strut is believed to play an important role. The blockage on the wing side of the wheels produced by this asymmetric component is expected to result in a pressure gradient between the wing and ground sides of the wheels.[2] Fluid traveling over the wing side of the fore wheel will follow the gradient through the wheel gap. On the ground side fluid is also moving into the gap, and the collision of these two flow regions results in a high degree of mixing. Flow through the wheel gap is expected to be even more prominent for a detailed fully functional landing gear because more structure on the wing side of the wheels should result in a stronger pressure gradient through the gap.

Error Sources and Estimation

DPIV measurements very near a boundary are often difficult and can result in data-acquisition errors. Reflections of the light sheet off the surface can produce flair or hot spots in the particle images and result in data dropout. For the current study test images were acquired while making light sheet and surface texture adjustments to ensure limited flair from the wheel surface. Another source of error during DPIV measurements is out-of-plane particle motion. Ideally, particles in the first image should travel a given distance before the second image is acquired, and the same particles captured in the first image should appear in the second. However, because of the finite thickness of the light sheet, transverse particle motion will result in velocity vector calculations that are clearly in error. To help eliminate this error, source adjustments were made to both the light sheet thickness and time between acquired images. As a check, the data images in a quadrant were reduced immediately after they were acquired to provide vector images. Ten percent of these vector images were then analysed to ensure that at least 90% of the

vectors in each were without obvious error before proceeding to data acquisition in the next quadrant.

For the current studies velocity vector determination required the calculation or measurement of three parameters. They included interrogation spot size, time delay Δt between acquired images in a pair, and pixel separation between the cross-correlation peaks. Uncertainty in the determination of the interrogation spot size is expected to be within ± 0.032 mm. Measurement of Δt was accomplished using photo sensors to detect the firing of each laser and an electronic counter to determine time between firings. According to the manufacturer, the electronic counter measures time differences with an accuracy of 500 ps. The DPIV image analysis software was designed to measure the separation between cross-correlation peaks with a subpixel accuracy of 0.1. To determine the propogation of uncertainty from the measurements into the presented results, the method of Kline and McClintock[6] was used. The following equation was derived to determine the percentage uncertainty in the velocity calculations:

$$\varepsilon_u/u = \left[(\varepsilon_{\text{iss}}/iss)^2 + (\varepsilon_{\text{dt}}/dt)^2 + (\varepsilon_{\text{px}}/px)^2\right]^{\frac{1}{2}}$$

Here the ε values are the uncertainty intervals for velocity u, the interrogation spot size iss the time differential between acquisition of images dt and separation between cross-correlation peaks px. Interrogation spot size remained constant throughout the study, and for the most part the time differential used was 4.1225 μs. With these values an uncertainty in the u velocity based on the freestream value is calculated to be approximately 4%. Using this result, calculation of mean velocity values is performed using the following equation:

$$\varepsilon_{\bar{u}} = \left[\left(\frac{\varepsilon_{u_1}\partial\bar{u}}{\partial u_1}\right)^2 + \left(\frac{\varepsilon_{u_2}\partial\bar{u}}{\partial u_2}\right)^2 + L + \left(\frac{\varepsilon_{u_n}\partial\bar{u}}{\partial u_n}\right)^2\right]^{\frac{1}{2}}$$

$$= \left(\frac{1}{n}\right)\sum_{i=1}^{n}\left(\varepsilon_{u_i}^2\right)^{\frac{1}{2}}$$

By assuming the value of ε_u is constant and knowing the value of n to be 100, the uncertainty in the mean velocity calculations is 1/10 of the uncertainty in the individual velocity calculations.

To determine the uncertainty in the calculation of the Reynolds stresses, we consider the following example equation for the calculation of the $\overline{u'^2}$ component:

$$\overline{u'^2} = \left(\frac{1}{n}\right)\left[(u_1-\bar{u})^2 + (u_2-\bar{u})^2 + L + (u_n-\bar{u})^2\right]$$

$$= \left(\frac{1}{n}\right)\sum_{i=1}^{n}(u_i-\bar{u})^2$$

From this we can determine an expression for the uncertainty:

$$\varepsilon_{\overline{u'^2}} = \left[\left(\frac{\varepsilon_{u_1}\partial\overline{u'^2}}{\partial u_1}\right)^2 + \left(\frac{\varepsilon_{\bar{u}}\partial\overline{u'^2}}{\partial\bar{u}}\right)^2 + \left(\frac{\varepsilon_{u_2}\partial\overline{u'^2}}{\partial u_2}\right)^2 + \left(\frac{\varepsilon_{\bar{u}}\partial\overline{u'^2}}{\partial\bar{u}}\right)^2\right.$$

$$\left. + L + \left(\frac{\varepsilon_{u_n}\partial\overline{u'^2}}{\partial u_n}\right)^2 + \left(\frac{\varepsilon_{\bar{u}}\partial\overline{u'^2}}{\partial\bar{u}}\right)^2\right]^{\frac{1}{2}}$$

Evaluating derivatives and assuming that the fluctuations are 10% of the mean, the preceding equation becomes

$$\varepsilon_{\overline{u'^2}} = \left\{2\left[\varepsilon_{u_i}(0.1\bar{u})\right]^2 + n\left[-2\varepsilon_{\bar{u}}(0.1\bar{u})\right]^2\right\}^{\frac{1}{2}}$$

Considering $\bar{u} = 29$ m/s and using the calculated values of ε_{u_i} and $\varepsilon_{\bar{u}}$, the uncertainty is determined to be 9.68 $(\text{m/s})^2$. In the region between the wheels where the mean w component of velocity was found to be 3 m/s with a standard deviation of 20 m/s, the error in the determination of $\overline{w'^2}$ is calculated to be 13%.

Conclusions

The current study examined the mean and fluctuating flowfields around a four-wheel landing gear. The model used was a simplified configuration with wheels and struts scaled to 31% of those on a Boeing 757. Dressings, wheel hubs, brake linings, and cross struts were eliminated. Tests were conducted at a Reynolds number based on wheel diameter of 6×10^5. Digital particle image velocity data were acquired and used to determine the mean components of velocity and Reynolds stress in the vertical midplane surrounding a set of in-line wheels.

The results highlight a region of significant turbulent activity in the gap between the wheels to the ground side of the wheel horizontal midplane. Turbulence production is expected to be high here as a result of flow pouring into the gap region from the wing and ground sides of the fore wheel. The mean transverse component of velocity in the gap is noted to be only about 10% of the freestream velocity, but the standard deviation is nearly 70% of the freestream velocity, indicating a highly unsteady region of flow. Transverse flow through the gap from the wing side of the wheels is expected to result from a vertical pressure gradient across the wheels because of blockage created by the center support strut. Gap flow is expected to be even more prominent for fully dressed landing gear because there is more wing-side structure to block the flow.

Acknowledgment

The author thanks C. Yao at the NASA Langley Research Center for providing information on particle-image-velocimetry data analysis.

References

[1]Hedges, L. S., Travin, A. K., and Spalart, P. R., "Detached-Eddy Simulations over a Simplified Landing Gear," *Journal of Fluids Engineering*, Vol. 124, June 2002, pp. 413–423.

[2]Lazos, B. S., "Mean Flow Features Around the Inline Wheels of a Four-Wheel Landing Gear," *AIAA Journal*, Vol. 40, No. 2, 2002, pp. 193–198.

[3]Lazos, B. S., "Surface Topology on the Wheels of a Generic Four-Wheel Landing Gear," *AIAA Journal*, Vol. 40, No. 12, 2002, pp. 2402–2411.

[4]Sellers, W. L., and Kjelgaard, S. O., "The Basic Aerodynamics Research Tunnel—A Facility Dedicated to Code Validation," AIAA Paper 88-1997, 1988.

[5]Landreth, C. C., and Adrian, R. J., "Measurements and Refinement of Velocity Data Using High Image Density Analysis in Particle Image Velocimetry," *Applications of Laser Anemometry to Fluid Mechanics: Proceedings of the 4th International Symposium*, edited by R. J. Adrian, T. Asunuma, D. Durão, F. Durst, and J. Whitlaw, Springer-Verlag, Berlin, 1988, pp. 484–497.

[6]Kline, S. J., and McClintock, F. A., "Describing Uncertainties in Single-Sample Experiments," *Mechanical Engineering*, Vol. 75, Jan. 1953, pp. 3–8.

W. Devenport
Associate Editor